Inorg. Chem. **2003**, *42*, 5531−5536

X-ray Absorption Spectroscopy of a Structural Analogue of the Oxidized Active Sites in the Sulfite Oxidase Enzyme Family and Related Molybdenum(V) Complexes

Farideh Jalilehvand,[†] Booyong S. Lim,[‡] R. H. Holm,*[,‡] Britt Hedman,*[,†,§] and Keith O. Hodgson*[,†,§]

Department of Chemistry, Stanford University, Stanford, California 94305, Stanford Synchrotron Radiation Laboratory, SLAC, Stanford University, Stanford, California 94309, and Department of Chemistry and Chemical Biology, Harvard University, Cambridge, Massachusetts 02138

Received January 29, 2003

X-ray absorption spectroscopy (XAS) (edge and extended X-ray absorption fine structure (EXAFS)) has been applied to the characterization of three molybdenum(V,VI) monodithiolene complexes with unidentate coligands, $[MoO(SC_6H_2\text{-}2,4,6\text{-}Pr^i_3)_2(bdt)]^-$ (**1**), $[MoOCl(SC_6H_2\text{-}2,4,6\text{-}Pr^i_3)(bdt)]^-$ (**2**), and $[MoO_2(SC_6H_2\text{-}2,4,6\text{-}Pr^i_3)(bdt)]^-$ (**3**) (bdt = benzene-1,2-dithiolate). These complexes are related to the active site in the xanthine oxidase and sulfite oxidase families and, as in the enzyme sites, bind monodentate thiolate. By comparison to the data of crystalline oxidized chicken sulfite oxidase, it is shown that complex **3**, whose thiolate simulates binding by the highly conserved cysteine, is an accurate structural analogue of the oxidized site of this enzyme. Normalized edge spectra, EXAFS data, Fourier transforms, and GNXAS-based fit results are presented. As in earlier studies, this provides characterization of new analogue complexes by XAS to facilitate identification of related sites in proteins.

Introduction

The Hille classification of molybdoenzymes recognizes three families designated according to their most prominent members: xanthine oxidase, sulfite oxidase, and dimethyl sulfoxide reductase.[1] In each family, the molybdenum atom is bound by one or two pterin−dithiolene cofactor ligands. The dimethyl sulfoxide reductase family is characterized by two pterin−dithiolene cofactor ligands bound to molybdenum in the reduced (desoxomolybdenum(IV)) and oxidized (monooxomolybdenum(VI)) forms. Structural analogues and functional analogue reaction systems in the form of bis(dithiolene)molybdenum(IV,V,VI) complexes have been achieved by recent research in these laboratories.[2−4] Because of the existence of molybdenum/tungsten isoenzymes,[5−7] the chemistry of bis(dithiolene)tungsten complexes has been developed in parallel.[8−13] In analogue species and, by inference, in protein sites, the cofactor ligand functions as a classical 1,2-dithiolate. An important component of this research is X-ray absorption spectroscopy (XAS) of a large inventory of complexes and analysis of extended X-ray absorption fine structure (EXAFS) spectra by the GNXAS protocol.[14,15]

Active sites in the sulfite oxidase and xanthine oxidase families contain a molybdenum atom bound by *one* pterin−dithiolene ligand. The approximately square pyramidal structures of the oxidized sites of chicken liver sulfite

* Authors to whom correspondence should be addressed. E-mail: hedman@ssrl.slac.stanford.edu (B.H.).
[†] Stanford Synchrotron Radiation Laboratory, SLAC, Stanford University.
[‡] Harvard University.
[§] Department of Chemistry, Stanford University.

(1) (a) Hille, R. *Chem. Rev.* **1996**, *96*, 2757−2816. (b) Hille, R. *Trends Biochem. Sci*. **2002**, *27*, 360−367. (c) Hille, R. *Met. Ions Biol. Syst*. **2002**, *39*, 187−226.
(2) Donahue, J. P.; Goldsmith, C. R.; Nadiminti, U.; Holm, R. H. *J. Am. Chem. Soc.* **1998**, *120*, 12869−12881.
(3) Lim, B. S.; Donahue, J. P.; Holm, R. H. *Inorg. Chem.* **2000**, *39*, 263−273.
(4) Lim, B. S.; Holm, R. H. *J. Am. Chem. Soc.* **2001**, *123*, 1920−1930.
(5) Buc, J.; Santini, C.-L.; Giordani, R.; Czjzek, M.; Wu, L.-F.; Giordano, G. *Mol. Microbiol.* **1999**, *32*, 159−168.
(6) Stewart, L. J.; Bailey, S.; Bennett, B.; Charnock, J. M.; Garner, C. D.; McAlpine, A. S. *J. Mol. Biol.* **2000**, *299*, 593−600.
(7) Garner, C. D.; Stewart, L. J. *Met. Ions Biol. Syst.* **2002**, *39*, 699−726.
(8) Lorber, C.; Donahue, J. P.; Goddard, C. A.; Nordlander, E.; Holm, R. H. *J. Am. Chem. Soc.* **1998**, *120*, 8102−8112.
(9) Goddard, C. A.; Holm, R. H. *Inorg. Chem.* **1999**, *38*, 5389−5398.
(10) Sung, K.-M.; Holm, R. H. *Inorg. Chem.* **2000**, *39*, 1275−1281.
(11) Sung, K.-M.; Holm, R. H. *J. Am. Chem. Soc.* **2001**, *123*, 1931−1943.
(12) Sung, K.-M.; Holm, R. H. *Inorg. Chem.* **2001**, *40*, 4518−4525.
(13) Sung, K.-M.; Holm, R. H. *J. Am. Chem. Soc.* **2002**, *124*, 4312−4320.
(14) Musgrave, K. B.; Donahue, J.; Lorber, C.; Holm, R. H.; Hedman, B.; Hodgson, K. O. *J. Am. Chem. Soc.* **1999**, *121*, 10297−10307.
(15) Musgrave, K. B.; Lim, B. S.; Sung, K.-M.; Holm, R. H.; Hedman, B.; Hodgson, K. O. *Inorg. Chem.* **2000**, *39*, 5238−5247.

10.1021/ic030039f CCC: $25.00
Published on Web 08/05/2003

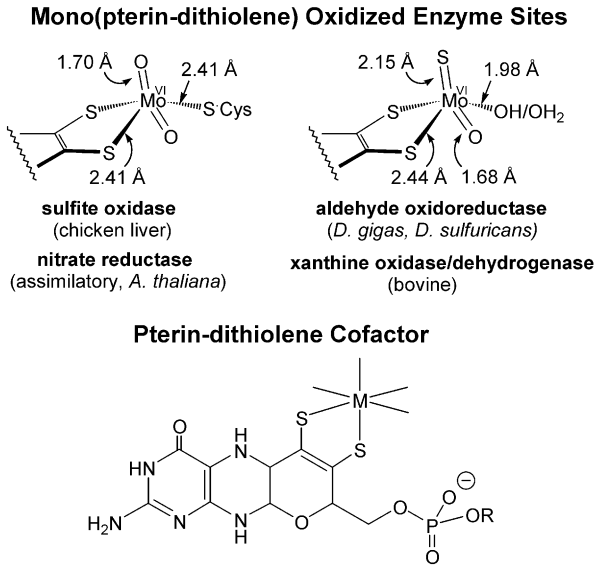

Figure 1. Depictions of the pterin−dithiolene cofactor ligand (R absent or a nucleotide) and oxidized active sites of members of the sulfite oxidase and xanthine oxidase enzyme families. Bond distances were determined by Mo EXAFS.[1a,21−23]

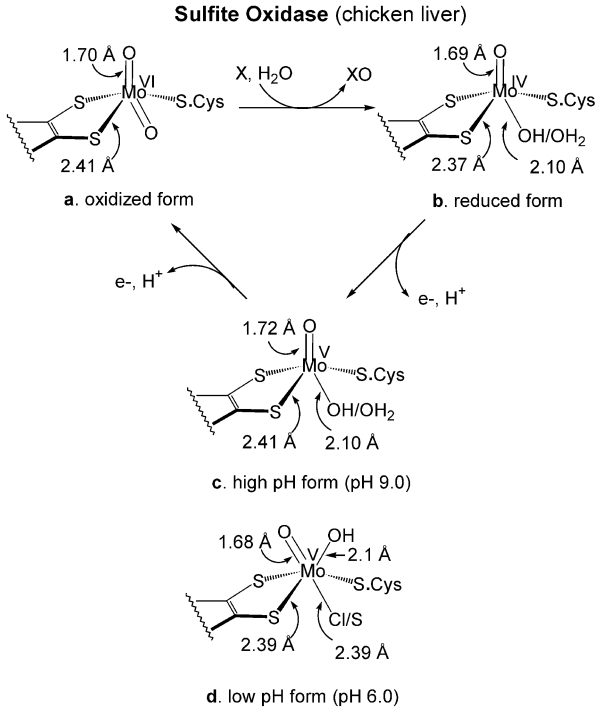

Figure 2. Site structures of the oxidized (a), reduced (b), high-pH (c), and low-pH (d) forms of sulfite oxidase.[1a,23]

oxidase[16] and bacterial aldehyde oxidoreductase,[17−20] a member of the xanthine oxidase family, have been crystallographically defined and are schematically depicted in Figure 1. A structural account of the sites in different forms of sulfite oxidase is presented in Figure 2. Bond distances in sulfite oxidase[21−23] and xanthine oxidase[1] follow from EXAFS analysis. Assimilatory nitrate reductase is a member of the xanthine oxidase family; the indicated structural information (Figure 1) was obtained from EXAFS analysis.[24] Crystal structures of sufficient accuracy to reveal one cofactor ligand but not the details of molybdenum coordination have been determined for bovine xanthine oxidase and dehydrogenase[25] and a bacterial xanthine dehydrogenase.[26] Functional enzymes in the sulfite oxidase family contain the $Mo^{VI}O_2$ unit. In the xanthine oxidase family, the presence of the Mo^{VI}-OS unit is essential to activity; the desulfo ($Mo^{VI}O_2$) form is inactive.[1] A third member of the xanthine oxidase family, carbon monoxide dehydrogenase, has been shown by crystallography to contain one pterin−dithiolene ligand.[27−29] In a unique structure, a Cu^{I} atom is coordinated to the sulfide ligand of the $Mo^{VI}OS$ unit.[29]

Metal monodithiolenes with unidentate coligands are an essentially unknown class of compounds. Very recently, we have initiated the synthesis of analogues of the active sites in the xanthine oxidase and sulfite oxidase families. A set of nine molybdenum(V,VI) monodithiolenes based on benzene-1,2-dithiolate (bdt) were prepared.[30] Here we examine the XAS of complexes **1**−**3** in Figure 3, which, as the enzyme sites, bind monodentate thiolate. As will be seen, complex **3**, whose thiolate simulates binding by the highly conserved cysteine in sulfite oxidase and assimilatory nitrate reductase, is an accurate structural analogue of the oxidized site of those enzymes. As in our earlier studies,[14,15] the intention of this work is the characterization of new analogue complexes by XAS to facilitate identification of related sites in proteins, especially in the absence of X-ray crystallographic information.

Experimental Section

Sample Preparation. The Et_4N^+ salts of $[MoO(SC_6H_2\text{-}2,4,6\text{-}Pr^i_3)_2(bdt)]^-$ (**1**), $[MoOCl(SC_6H_2\text{-}2,4,6\text{-}Pr^i_3)(bdt)]^-$ (**2**), and $[MoO_2(SC_6H_2\text{-}2,4,6\text{-}Pr^i_3)(bdt)]^-$ (**3**) were prepared as described.[30] The solid samples were ground to fine powders in a glovebox under a

(16) Kisker, C.; Schindelin, H.; Pacheco, A.; Wehbi, W. A.; Garrett, R. M.; Rajagopalan, K. V.; Enemark, J. H.; Rees, D. C. *Cell* **1997**, *91*, 973−983.
(17) Romão, M. J.; Archer, M.; Moura, I.; Moura, J. J. G.; LeGall, J.; Engh, R.; Schneider, M.; Hof, P.; Huber, R. *Science* **1995**, *270*, 1170−1176.
(18) Huber, R.; Hof, P.; Duarte, R. O.; Moura, J. J. G.; Moura, I.; Liu, M.-Y.; LeGall, J.; Hille, R.; Archer, M.; Romão, M. J. *Proc. Natl. Acad. Sci. U.S.A.* **1996**, *93*, 8846−8851.
(19) Rebelo, J.; Maceira, S.; Dias, J. M.; Huber, R.; Ascenso, C. S.; Rusnak, F.; Moura, J. J. G.; Moura, I.; Romão, M. J. *J. Mol. Biol.* **2000**, *297*, 135−146.
(20) Rebelo, J. M.; Dias, J. M.; Huber, R.; Moura, J. J. G.; Romão, M. J. *J. Biol. Inorg. Chem.* **2001**, *6*, 791−800.
(21) George, G. N.; Garrett, R. M.; Prince, R. C.; Rajagopalan, K. V. *J. Am. Chem. Soc.* **1996**, *118*, 8588−8592.
(22) George, G. N.; Pickering, I. J.; Kisker, C. *Inorg. Chem.* **1999**, *38*, 2539−2540.
(23) George, G. N.; Kipke, C. A.; Prince, R. C.; Sunde, R. A.; Enemark, J. H.; Cramer, S. P. *Biochemistry* **1989**, *28*, 5075−5080.
(24) George, G. N.; Mertens, J. A.; Campbell, W. H. *J. Am. Chem. Soc.* **1999**, *121*, 9730−9731.
(25) Enroth, C.; Eger, B. T.; Okamoto, K.; Nishino, T.; Nishino, T.; Pai, E. F. *Proc. Natl. Acad. Sci. U.S.A.* **2000**, *97*, 10723−10728.
(26) Truglio, J. J.; Theis, K.; Leimkühler, S.; Rappa, R.; Rajagopalan, K. V.; Kisker, C. *Structure* **2002**, *10*, 115−125.
(27) Dobbek, H.; Gremer, L.; Meyer, O.; Huber, R. *Proc. Natl. Acad. Sci. U.S.A.* **1999**, *96*, 8884−8889.
(28) Hänzelmann, P.; Dobbek, H.; Gremer, L.; Huber, R.; Meyer, O. *J. Mol. Biol.* **2000**, *301*, 1221−1235.
(29) Dobbek, H.; Gremer, L.; Kiefersauer, R.; Huber, R.; Meyer, O. *Proc. Natl. Acad. Sci. U.S.A.* **2002**, *99*, 15971−15976.
(30) Lim, B. S.; Willer, M. W.; Miao, M.; Holm, R. H. *J. Am. Chem. Soc.* **2001**, *123*, 8343−8349.

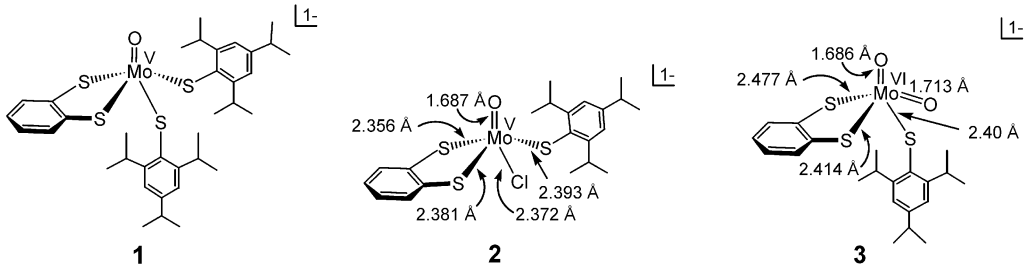

Figure 3. Schematic structures of **1**−**3** with the indicated bond lengths. Structures **2** and **3** have been determined crystallographically;[30] complex **1** is considered to have analogous square pyramidal geometry, with distances determined from the present EXAFS study.

dinitrogen atmosphere, and diluted with boron nitride to obtain $\Delta\mu x \leq 1$ over the absorption edge and to reduce self-absorption. The mixtures were pressed into pellets and sealed between 63 μm Kapton windows in a 1 mm aluminum spacer. The samples were frozen in liquid nitrogen immediately upon removal from the glovebox and kept at this or a lower temperature throughout storage and data collection.

XAS Data Collection. X-ray absorption spectra were measured for all samples at beam line 7-3, Stanford Synchrotron Radiation Laboratory (SSRL), under operating conditions of 3.0 GeV and 100−70 mA, and with a Si(220) double-crystal monochromator tuned at 21549 eV. An Oxford Instrument CF1208 continuous-flow liquid helium cryostat was used to maintain a constant sample temperature of 10 K. The Mo K-edge XAS data were collected in transmission mode to $k = 20$ Å^{-1} with argon as the absorbing gas in the ionization chamber detectors. Internal energy calibration was performed by simultaneous measurement of the K-edge of a Mo foil placed between the second and third ionization chambers, assigning the first inflection point to 20003.9 eV. The data represent averages of 8, 18, and 22 scans for complexes **1**, **2**, and **3**, respectively.

XAS Data Analysis. The ab initio GNXAS method was used in the data analysis. The theoretical basis for the GNXAS approach and its fitting methodology have been described in detail elsewhere.[31−33] Theoretical EXAFS signals were generated for an initial structural model based on the crystallographic coordinates[30] for the corresponding complexes (**2** and **3**, Figure 3) up to a distance cutoff of 5.0 Å. Phase shifts calculated according to the standard muffin-tin approximation were used to generate the separate two- and three-body EXAFS signals. GNXAS fits of this model were performed using averaged raw absorption data over the k range 3.4−17.6 Å^{-1} by a least-squares minimization procedure that includes the MINUIT subroutine of the CERN library. The quality of the fits was compared by means of the least-squares residual $\mathcal{R}$, and monitored by visual inspection of the fits to the data and their Fourier transforms (FTs), and of the residual EXAFS signal and its FT. The structural parameters varied during the refinements were the bond distance (R) and the bond variance (σ_R^2) for the two-body signals. The σ_R^2 parameter is related to the Debye−Waller factor, which is a measure of thermal vibration and the static disorder of the absorber/scatterers. The nonstructural parameters E_0 and S_0^2 were varied, whereas Γ_C (core hole lifetime) and E_r (experimental resolution) were kept fixed to physically reasonable values throughout the analysis. The coordination numbers were set to the values determined by X-ray crystallography. All parameters were varied within a preset range, and all results were checked to ensure that the values obtained did not reach the high or low points of these fitting ranges.

Results and Discussion

Molybdenum K-Edge Spectra. The energy position of the molybdenum K-edge is sensitive to the electronic structure of the absorber, and the formal or effective oxidation state can often be determined from the edge spectrum. Figure 4a shows the normalized Mo K-edge spectra of complexes **1**−**3**. The edge shapes of the spectra for **1** and **2** are almost identical over a wide energy range, with the edge position of **2** displaced ∼1.2 eV to higher energy. The spectrum of **3** is shifted by ∼2.7 eV to higher energy relative to that of **2**. This is consistent with a difference in formal oxidation state, i.e., +5 for **1** and **2** and +6 for **3**, as well as the replacement of a thiolate by a more electronegative ligand.

The pre-edge feature at ∼20012 eV is most pronounced for complex **3**. This feature is characteristic of the presence of a Mo═O group and originates from a formally dipole-forbidden 1s → 4d excitation to antibonding orbitals directed principally along the Mo═O bond.[34] The edge spectrum of **3** strongly overlaps that of crystalline oxidized chicken sulfite oxidase[22] (Figure 4b), indicating very close agreement in geometry and oxidation state for the Mo sites, and the presence of a dioxo ($Mo^{VI}O_2$) moiety in both centers.

EXAFS Analysis. The EXAFS data for complexes **1**−**3** are compared in Figure 5a. Those of complexes **1** and **2** are very similar, while the amplitude of the EXAFS oscillations for **3** is considerably smaller. This reflects the lower number of sulfur/chloride ligands and higher number of oxygens as backscatterers, as well as a destructive interference between the Mo−S/Cl and Mo−O waves in the EXAFS, which increases with the higher ratio of O/S in **3** (cf. Figure S1 in the Supporting Information).

Two distinct peaks are observed in the FTs of all three complexes (Figure 5b), corresponding to the Mo−O and Mo−S/Cl waves. The FTs for complexes **1** (for which the fits to the EXAFS data establish that the Mo atom is coordinated by four S atoms and one O atom; see below) and **2** (with Mo surrounded by three S atoms, one Cl atom, and one O atom) are almost identical in peak position and

(31) Filipponi, A.; Di Cicco, A.; Tyson, T. A.; Natoli, C. R. *Solid State Commun.* **1991**, *78*, 265−268.
(32) Filipponi, A.; Di Cicco, A.; Natoli, C. R. *Phys. Chem. Rev. B* **1995**, *52*, 15122−15134.
(33) Westre, T. E.; Di Cicco, A.; Filipponi, A.; Natoli, C. R.; Hedman, B.; Solomon, E. I.; Hodgson, K. O. *J. Am. Chem. Soc.* **1995**, *117*, 1566−1583.
(34) Kutzler, F. W.; Natoli, C. R.; Misemer, D. K.; Doniach, S.; Hodgson, K. O. *J. Chem. Phys.* **1980**, *73*, 3274−3288. (b) Kutzler, F. W.; Scott, R. A.; Berg, J. M.; Hodgson, K. O.; Doniach, S.; Cramer, S. P.; Chang, C. H. *J. Am. Chem. Soc.* **1981**, *103*, 6083−6088.

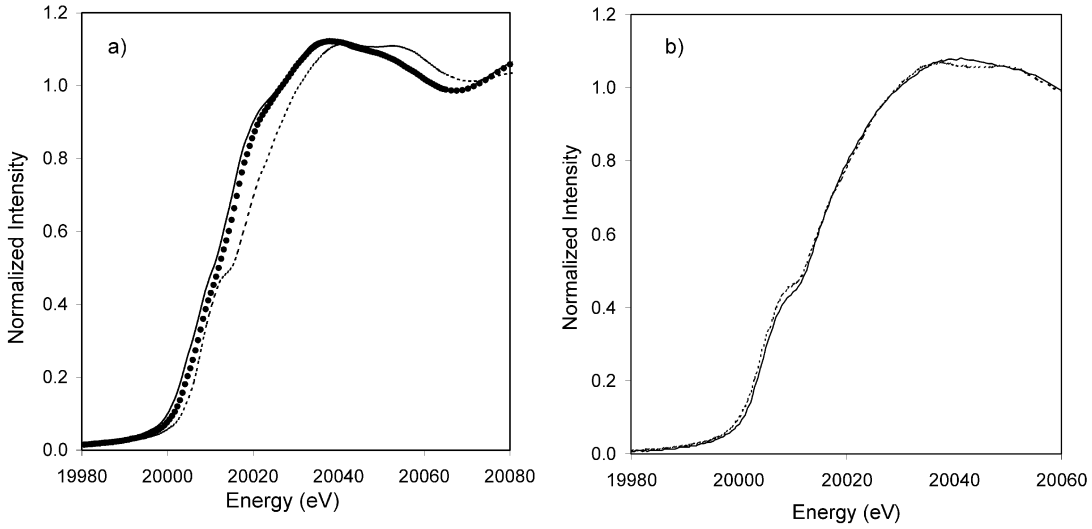

Figure 4. (a) Normalized Mo K-edge spectra of **1** (···), **2** (—), and **3** (---). (b) Comparison of the normalized Mo K-edge spectra of **3** (---) and crystalline oxidized chicken sulfite oxidase from ref 22 (—; data provided by Dr. G. N. George) showing the very strong overlap in edge structures.

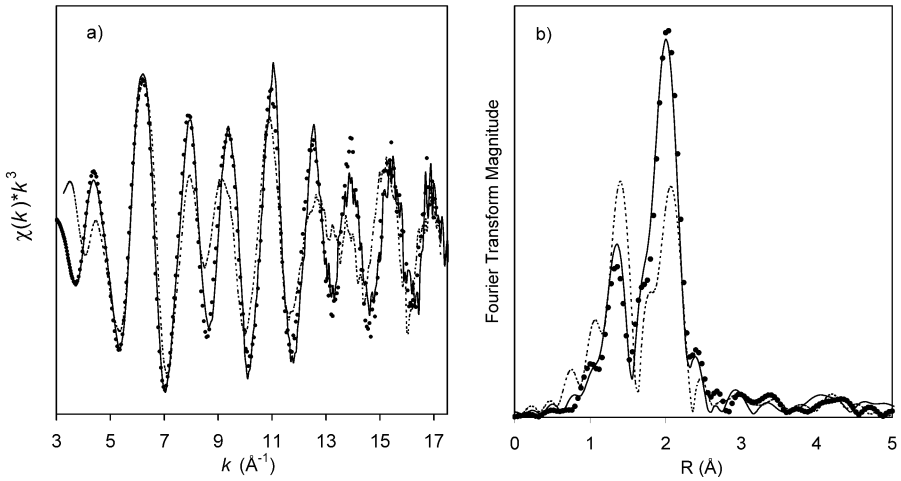

Figure 5. Comparison of the (a) EXAFS spectra and (b) non-phase-shift-corrected Mo K-edge Fourier transforms of **1** (···), **2** (—), and **3** (---).

intensity, reflecting the similarity in structure at the Mo center, and the closely related phase and amplitude functions of sulfur and chlorine backscatterers in the EXAFS. This is consistent with the X-ray crystallographic results for **2**, which show that the bond distances are very close, i.e., Mo−Cl = 2.372 Å, Mo−S_{bdt} = 2.37 Å, and Mo−$S_{thiolate}$ = 2.393 Å.[30] The intensity of the Mo−O peak for complex **3**, which contains the signal from two Mo═O groups, is higher than those of **1** and **2,** and slightly shifted to higher *R* values. This effect could be caused by the small difference in the Mo═O bond distances, as determined from the crystal structures. The Mo−S FT peak intensity for complex **3** with three sulfur ligands is almost 40% lower than those of **1** and **2**. This results not only from the smaller number of S/Cl ligands, but also from the larger distribution in Mo−S distances (2.40−2.48 Å).

GNXAS least-squares fits were performed using calculated phase and amplitude functions for models based on the crystallographic coordinates of **2** and **3**. The individual contributions for separate scattering pathways for complexes **1**−**3** included in the fits and the experimental data are shown in Figure S1, and the fit results are given in Table 1. The mean interatomic Mo−X distances are, within the estimated error of ±0.02 Å, in agreement with the mean values from the crystallographic results for **2** and **3**. For complex **1**, whose crystal structure is unknown, the EXAFS fit results establish that it has a first-shell coordination sphere of one O atom at 1.69 Å and four S atoms at an average distance of 2.41 Å. Figure S2 in the Supporting Information represents the corresponding Fourier transforms of the experimental data, fits, and FTs of the fit residuals for all three complexes.

The Mo−O and Mo−S/Cl single scattering pathways dominate the EXAFS signals, and the Fourier transforms show that other contributions are minor. Introduction of three-body pathways gave in general no significant improvement, although the presence of some multiple scattering is seen in the residual. For complex **2** an additional low-intensity FT peak visible above the noise level at about 3.0 Å could indeed be successfully fit as a Mo−C_{bdt} interaction. For this complex two different fitting models were in addition tested. The first model includes the crystallographically determined three Mo−S, one Mo−Cl, and two Mo−C_{bdt} scattering paths, whereas the second assumed four Mo−S/Cl (fit as Mo−S) and two Mo−C_{bdt} interactions. The fit

Table 1. GNXAS Fit Results of Mo K-Edge EXAFS Analysis[a]

	Mo−O			Mo−S			additional contributions				
	N	*R* (Å)	σ^2 (Å^2)	*N*	*R* (Å)	σ^2 (Å^2)		*N*	*R* (Å)	σ^2 (Å^2)	$\mathscr{R}$
1	1	1.69	0.0016	4	2.41	0.0017					1.10×10^{-7}
2 model I	1	1.69	0.0009	3	2.38	0.0025	Mo−Cl	1	2.40	0.0011	1.19×10^{-7}
							Mo−C	2	3.29	0.0090	
model II	1	1.69	0.0009	4	2.40	0.0022	Mo−C	2	3.29	0.0091	1.19×10^{-7}
3	2	1.72	0.0010	3	2.45	0.0029					1.26×10^{-7}

[a] The coordination numbers (*N*) were fixed, while the distance (*R*) and disorder parameters σ^2 were allowed to float. The S_0^2 (0.85, 0.90, 0.80) and E_0 (20016.4, 20014.6, 20018.0 eV) values were also refined for **1**, **2**, and **3**, respectively.

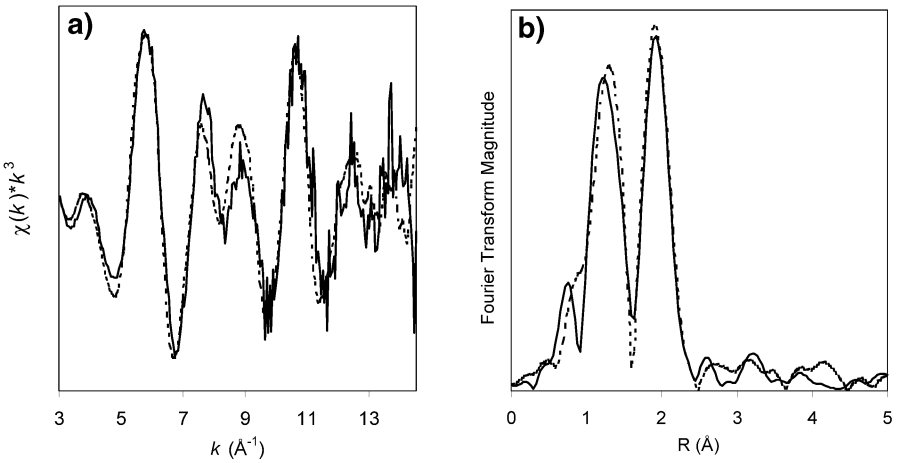

Figure 6. Comparison of (a) EXAFS data and (b) Fourier transforms of crystalline oxidized chicken sulfite oxidase (—) and **3** (---). The E_0 value for **3** has been modified to match that of the enzyme data. The data are within noise strongly similar and confirm the analogy in structure of the two centers. The enzyme data were provided by Dr. G. N. George.[22]

residual function $\mathscr{R}$ is the same for both models (Table 1), confirming the inability of the EXAFS technique to distinguish directly between two very close Mo−X distances involving ligands (S and Cl) that have very similar backscattering parameters. However, in the first model, the σ^2 parameter attained a reasonably low value for the strongly coordinated single chloride ligand. For sulfur the first model gave a larger σ^2 value, resulting from the distribution of the different Mo−S bond distances, whereas for the second model the σ^2 value represented the overall distribution of the four Mo−ligand distances (Mo−Cl = 2.372 Å; Mo−S_{bdt} = 2.356, 2.382 Å; Mo−$S_{thiolate}$ = 2.393 Å).[30] For complex **3**, the even wider spread of the Mo−S distances, from 2.40 to 2.48 Å (cf. Figure 3), is reflected in the even larger σ^2 value (Table 1), while the relatively small σ^2 value for **1** indicates a much smaller spread in its four Mo−S bond distances. The low residuals in both *k*- and *R*-space show that the models used are satisfactory without inclusion of any additional paths.

Conclusion

Mo K-edge X-ray absorption spectra of three monodithiolenemolybdenum complexes with unidentate thiolate coligands have been examined. Complexes **1** and **2** approach the proposed structure of the high-pH form of sulfite oxidase, and complex **3** is an analogue of the oxidized active sites in the enzymes sulfite oxidase and assimilatory nitrate reductase. GNXAS fits to the EXAFS data for **2** and **3** agree (within ±0.02 Å) with those obtained from crystallographic studies, whereas the structure for complex **1** is determined from EXAFS to be very closely analogous to that of **2**. This is also confirmed from the Mo K-edge structure, which is close to identical for **1** and **2**.

The edge structure can clearly distinguish between 5-coordinate structures containing one and two oxygen ligands, and also shows explicit sensitivity for the Mo^V and Mo^{VI} oxidation states. The EXAFS data similarly have interference pattern characteristics that readily can delineate a 4 + 1 from a 3 + 2 (S + O) coordination. Comparison of data for complex **3** with those of crystallized oxidized chicken sulfite oxidase show that both the edge (Figure 4b) and EXAFS (Figure 6) data are superimposable within the noise, and thus confirm the validity of complex **3** as an accurate representation of the active site in that enzyme.

This work has afforded structural characterization of new analogue complexes by XAS. It is part of a series of investigations[14,15] intended to facilitate identification of related sites in molybdoenzymes, especially in the absence of X-ray crystallographic information.

Acknowledgment. This research was supported by NSF Grant CHE 98-76457 (R.H.H) and NIH Grant RR-01209 (K.O.H). Stanford Synchrotron Radiation Laboratory operation is funded by the U.S. Department of Energy, Office of Basic Energy Sciences. The SSRL Structural Molecular Biology Program is supported by the Department of Energy, Office of Biological and Environmental Research, and by the National Institutes of Health, National Center for Research Resources, Biomedical Technology Program. We

thank Dr. Graham N. George, SSRL, for making available the chicken sulfite oxidase XAS data.

Supporting Information Available: EXAFS fits and experimental data including the contribution of the individual scattering paths and the fit residual and Fourier transforms of the data and fits including the residual, all for complexes **1**−**3**. This material is available free of charge via the Internet at http://pubs.acs.org.

IC030039F